Copper Interconnects: Surface State Engineering to Facilitate Specular Electron Scattering

Erik Milosevic and Daniel Gall

***Abstract*— *In situ* electron transport measurements on epitaxial 10-nm-thick Cu(001) with Al and AlO_x cap layers indicate that the electron surface scattering specularity increases when the density of electronic surface states decreases. The Cu layers were sputter deposited on MgO(001) substrates and their resistance measured *in situ* as a function of the Al cap thickness d_{Al} = 0 - 1.4 nm as well as oxygen exposure from 10^{-1} to 10^5 Pa·s. The resistance increases with increasing d_{Al}, indicating a decrease in the surface scattering specularity that is well described by an exponential decay, attributed to the linearly increasing number of localized surface states available for electron scattering. In contrast, exposure to 0.04 - 50 Pa O_2 results in a decrease in the measured resistance as the Al cap is oxidized to form AlO_x, leading to a decreasing surface density of states and increasing scattering specularity with increasing x. The conductance enhancement is most pronounced for d_{Al} = 0.4 nm, since a larger d_{Al} leads to incomplete Al oxidation while a smaller d_{Al} insufficiently suppresses copper surface oxidation, causing a transition to diffuse surface scattering. The overall results indicate that insulating liner layers provide a conductance advantage for narrow interconnect lines.**

***Index Terms*—Interconnects, Copper, BEOL, MOL, Resistivity Scaling, Mean Free Path, Surface Scattering, Specularity**

I. Introduction

ELECTRON transport in metallic conductors with reduced dimensions remains a topic of considerable interest to the semiconductor industry because the resistivity of narrow interconnect wires strongly affects the speed and power consumption of integrated circuits [1]–[4]. At dimensions roughly equivalent to, or smaller than the electron mean free path in the bulk, electron scattering at surfaces [5]–[7], grain boundaries [8]–[12], and surface roughness [13]–[15] cause the resistivity to be well above the bulk value. For example, Cu with a mean free path λ = 39 nm [16] exhibits a 400% resistivity increase as the wire cross-sectional area is decreased to 400 nm^2 [17].

Electron scattering at surfaces is typically quantified using the classical model by Fuchs and Sondheimer (FS) [18], [19], who describe electron-surface interactions phenomenologically using a specularity parameter p that adopts a value between 0 and 1. Zero specularity (p = 0) corresponds to completely diffusive scattering where the electron momentum is randomized upon scattering at the surface, resulting in a resistivity increase. Conversely, specular scattering (p = 1) corresponds to electron reflection from the surface with conservation of the parallel momentum component and, therefore, no effect on the resistivity. Thus, metal surfaces/interfaces that exhibit a large electron scattering specularity are desired for next generation interconnect technologies. Surfaces with partially specular electron scattering have been reported for Cu [7], Ag [20], Au [21]–[23], and Co [24]. The most common interconnect material is Cu, for which a specularity of p = 0.6 – 0.7 has been reported at the Cu-vacuum interface [7], [25], [26]. However, exposure of the Cu surface to an oxygen-containing atmosphere causes a transition to completely diffuse electron scattering which is attributed to oxide formation and the related atomic level surface roughness [27]. Similarly, most studies report p = 0 for the interface between Cu and barrier layers such as Ti [28] and TiN [29], while there is still some disagreement regarding the industrially most relevant Cu-Ta interface [7], [28], [30], which may be attributed to the difficulty in deconvoluting the effects of surface and grain boundary scattering [6], [31]. Some evidence for non-zero (partial) specular electron scattering has been reported for interfaces of Cu with SiO_2 [32], Ni/NiO [25], TiO_2 [26], AlO_x and TaO_x [33], suggesting that oxide barriers may be more likely to facilitate specular scattering at the Cu-barrier interface than metallic layers. This is also consistent with the reported decrease of Al and Ti coated Cu layers upon atmospheric exposure [26], [33], which is attributed to a reduction in the local surface density of states (LDOS) at the Fermi level upon oxidation [26].

In this study, we investigate the electron scattering at the Cu-metal vs Cu-insulator interfaces for the Cu-Al/AlO_x system using continuous *in situ* transport measurements during O_2 adsorption and oxidation of Al capping layers on nominally 10-nm-thick epitaxial Cu(001) films grown on MgO(001). The use of epitaxial films allows quantification of electron surface

The authors acknowledge funding from SRC under task 2881, the NY State Empire State Development's Division of Science, Technology and Innovation (NYSTAR) through Focus Center-NY–RPI Contract C150117, and the NSF under grant No. 1740271 and 1712752.

The authors are from The Department of Materials Science and Engineering, Rensselaer Polytechnic Institute, 110 8th St, Troy, NY 12180, USA.

scattering without the confounding effects from scattering at grain boundaries. The results show an exponential decay in the scattering specularity with increasing Al capping layer thickness d_{Al} = 0 - 1.4 nm. Conversely, Cu coated with 0.4 nm Al shows an increase in specularity upon oxygen exposure which is attributed to oxidation of the Al cap and protection of the Cu underlayer from oxidation. The resulting AlO_x coated Cu has a higher conductance than oxygen-exposed bare Cu, demonstrating the promise of this approach to design barrier layers for narrow high conductivity interconnects.

II. Procedure

The Cu(001) layers and Al capping layers were deposited in a three-chamber ultra-high vacuum DC magnetron sputtering system with a base pressure of 10^{-7} Pa [34]. Polished 10 × 10 × 0.5 mm^3 MgO(001) substrates were cleaned ultrasonically in consecutive baths of trichloroethylene, acetone, isopropyl alcohol, and deionized water, mounted to a Mo stub with colloidal silver paint, and inserted into the deposition system through a load lock. Substrates were degassed *in situ* at 1000 °C for one hour and allowed to cool to room temperature during approximately 12 h. 5-cm-diameter Cu (99.999%) and Al (99.99%) targets were positioned facing the substrate at 45° at a distance of 9 cm and were sputter-cleaned with closed shutters for 5 min. Cu depositions were done in 0.40 ± 0.03 Pa Ar (99.999%) with a continuously rotating substrate at room temperature (298 K). A constant magnetron power of 40 W yielded a deposition rate of 0.25 nm/s, resulting in a nominal thickness of 10 nm for the Cu layers deposited for 40 seconds. The films were transferred *in situ* to an attached analysis chamber for *in situ* resistance measurements using a linear four-point probe operated at 1-100 mA. Subsequently, samples were transferred back to the deposition chamber without air exposure for deposition of Al cap layers at 298 K in 0.93 ± 0.04 Pa Ar using a magnetron power of 40 W and a ported shutter to limit the Al deposition rate to 0.002 nm/s. The deposition time of 0, 55, 220, or 672 seconds was chosen to obtain a set of samples with varying Al capping layer thicknesses d_{Al} = 0 - 1.4 nm, as determined from deposition rate calibrations and confirmed by X-ray reflectivity analyses. The capped Cu layers were then moved to the analysis chamber for additional *in situ* transport measurements, including the effect of oxygen exposure. This was done by continuously measuring the resistivity while introducing a constant flux of a 90%Ar – 10%O_2 gas mixture. During these oxidation experiments, the valves to the vacuum pumps were closed, leading to a chamber pressure that increases linearly by 0.08 Pa/s, reaching a 500 Pa total pressure corresponding to a 50 Pa O_2 partial pressure at the end of a ~1.6 h experiment. Finally, the samples were removed from the system via a load lock and their *ex situ* sheet resistances measured after air exposure (15-25% relative humidity) using a second four-point probe set up.

X-ray diffraction (XRD) and X-ray reflectivity (XRR) analyses were performed using a PANalytical X'pert PRO MPD system with a Cu source and a parabolic mirror yielding a parallel beam with <0.055° divergence, and a 0.27° parallel plate collimator in front of a scintillation point detector. XRR data was fit using the PANalytical X'Pert Reflectivity software, which makes use of the Parratt formalism for reflectivity. For this purpose, the densities of MgO, Cu, and Al are fixed at the known values of 3.58, 8.92, and 2.17 g/cm^3, respectively. Similarly, the density of the copper surface oxide was assumed to match the bulk Cu_2O density of 6.0 g/cm^3 and the surface AlO_x density was fixed to 3 g/cm^3, the reported value for the native oxide layer on Al [35].

III. Results and Discussion

All Cu layers in this study are epitaxial Cu(001)/MgO(001) layers. The epitaxy is confirmed with XRD methods [5], [26], [36], [37] using a combination of ω-2θ scans, ω rocking curves and φ-scans of the Cu(311) reflections. The Cu layer microstructure including misfit dislocation density and interface structure is similar to what we have previously reported in [38]–[40]. Fig. 1 shows representative XRR analyses from two nominally 10-nm-thick Cu(001) films, one without Al coating (d_{Al} = 0 nm) and one coated with Al for 672 s, yielding d_{Al} = 1.4 nm. The measured intensity is plotted as solid lines in a logarithmic scale as a function of the scattering angle 2θ, while the results from curve fitting are shown as dotted lines, offset by a factor of $\times 10^2$ above their respective experimental data for clarity purposes. The curve from the Cu film with d_{Al} = 0 nm is best described by a 9.1 ± 0.3 nm thick Cu layer with a 0.5 ± 0.2 nm CuO_x surface oxide, consistent with previously reported thin native Cu_2O layers on epitaxial Cu [26].

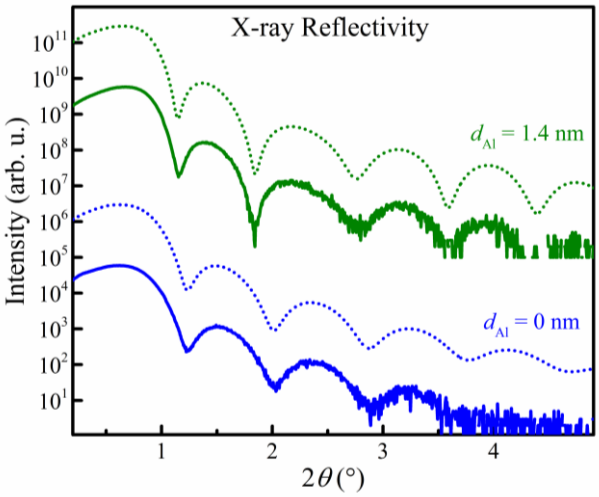

Fig. 1. Representative XRR analyses from 9.4-nm-thick Cu(001) (blue) and from 10.3-nm-thick Cu(001) with an Al capping layer with thickness d_{Al} = 1.4 nm (green). The dotted lines are the results from curve fitting

We use these two values to determine the as-deposited *in situ* film thickness d_{Cu} = 9.4 nm from the sum of the measured 9.1 nm and the equivalent thickness of 0.3 nm of metallic Cu contained within the measured 0.5 nm CuO_x layer. The curve fitting also provides values for the root-mean-square (RMS) roughness of the CuO_x surface of 0.25 ± 0.15 nm, as well as the interface roughnesses of 1.4 ± 0.5 and 0.6 ± 0.1 nm for the CuO_x-Cu and Cu-MgO interfaces, respectively. We note that the XRR analysis does not provide lateral information about the

Cu surface morphology, but that we expect it to be comparable to what we have previously reported for Cu layers deposited in the same deposition system [39]. The Al-coated Cu layer (green color in Fig. 1) exhibits a measured intensity which is best fit with a Cu thickness d_{Cu} = 10.3 ± 0.1 nm, no CuO_x layer, and a partially oxidized Al cap consisting of a 1.0 ± 0.1 nm thick metallic Al layer in direct contact with the Cu and an Al surface oxide with thickness d_{AlOx} = 0.7 ± 0.2 nm. The latter two values yield a total *in situ* deposited Al thickness of 1.4 nm, determined using the equivalent metallic Al thickness (0.4 nm) from the surface oxide. This corresponds to a measured Al deposition rate of 0.0021 nm/s, in good agreement with 0.0018 nm/s from another sample and 0.0020 nm/s from deposition rate calibrations using an 8-nm-thick Al sample deposited on SiO_2. The measured d_{Cu} = 10.3 nm corresponds to the as-deposited Cu thickness, since the Al cap protects the underlying Cu such that no Cu is consumed due to surface oxidation. The RMS roughness values from the plotted XRR curve are 0.5 ± 0.1, 0.7 ± 0.2, 0.55 ± 0.05, and 0.15 ± 0.08 nm for the AlO_x surface and the AlO_x-Al, Al-Cu, and Cu-MgO interfaces, respectively. We note that the measured oxide thickness of 0.7 nm matches the terminal thickness reported for Al(111) exposed to 4×10^{-5} Pa oxygen, but is smaller than for larger O_2 pressures [41]. The exact reasons for this disagreement are not known, but may be related to the particular epitaxial Al(001)/Cu in our study and the related charge transfer, strain, and/or absence of nucleation sites for layer-by-layer oxide formation [41]. Similar XRR analyses are done for two additional samples, both with a nominally identical d_{Cu} = 10 nm but with shorter Al deposition times of 55 and 220 s, leading to nominal Al thicknesses of d_{Al} = 0.1 and 0.4 nm, as also summarized in Table I. An Al cap thickness of 0.1 nm corresponds to approximately half a monolayer, such that the developing surface oxide is expected to be a mixed Cu/Al-oxide. XRR fitting indicates that this oxide is 1.3 ± 0.3 nm thick and has a density of 3.5 ± 0.5 g/cm^3, which lies (as expected) between the values for native AlO_x (3 g/cm^3) and Cu_2O (6.0 g/cm^3). XRR fitting of the sample with d_{Al} = 0.4 nm yields d_{Cu} = 10.1 ± 0.2 nm and an AlO_x thickness of 0.7 ± 0.2 nm with no metallic Al or Cu_2O layers. That is, XRR indicates that the 0.4 nm thick metallic Al cap layer is completely oxidized in air, but that the developing AlO_x at the surface inhibits oxidation of the Cu underlayer.

TABLE I

AS-DEPOSITED		AIR-EXPOSED	
d_{Cu} (nm)	d_{Al} (nm)	Surface layer	d (nm)
9.4	0	CuO_x	0.5
10.0	0.1	CuO_x-AlO_x	1.3
10.1	0.4	AlO_x	0.7
10.3	1.4	Al + AlO_x	1.0 + 0.7

As-deposited thickness d_{Cu} of Cu layers and d_{Al} of Al cap layers, and surface oxide type and thickness after air-exposure, as determined by XRR measurements from four samples.

Fig. 2 is a plot of the measured sheet resistance R_s vs processing step from four samples with varying Al cap thickness d_{Al} = 0-1.4 nm. As indicated by the *x*-axis labels, R_s is measured *in situ* after Cu(001) deposition, *in situ* after subsequent Al deposition, during controlled O_2 exposure over six orders of magnitude from 0.1 to 1.5×10^5 Pa·s, and *ex situ* after air-exposure. The first four data points labeled "Bare Cu" are the *in situ* measured sheet resistance from the four samples directly after Cu deposition. Their values R_s = 3.33 ± 0.09, 3.62 ± 0.11, 3.34 ± 0.10 and 3.70 ± 0.11 Ω/□ yield an average R_s = 3.50 ± 0.16 Ω/□. The latter stated uncertainty corresponds to the standard deviation of 4.6 % for the resistance of these four Cu layers which are deposited under nominally identical conditions but may exhibit variations in crystalline quality, thickness, interface structure, and surface roughness. The fact that the standard deviation is relatively small is an indication of the good experimental reproducibility of the epitaxial Cu(001) deposition. We also determine the resistivity ρ from these four Cu layers, using the measured R_s and as-deposited d_{Cu} of each sample, and determine an average ρ = 3.48 ± 0.26 μΩcm. This value is 2.1 times larger than the bulk Cu resistivity, which is attributed to electron scattering at the Cu surface and the Cu-MgO interface, and is in reasonable agreement with the reported ρ = 3.82 μΩcm of epitaxial Cu(001) with d_{Cu} = 9.3 nm [26].

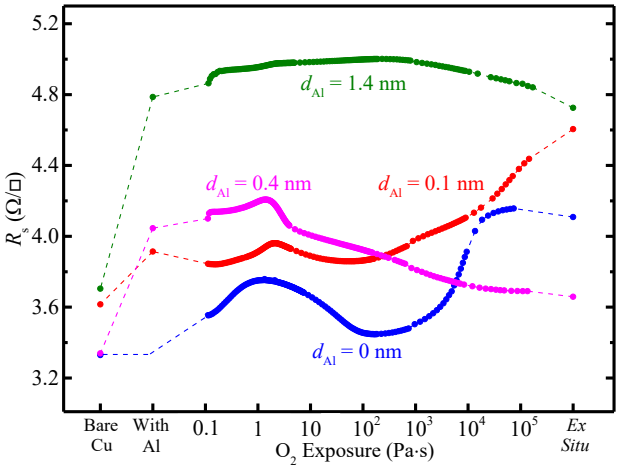

Figure 2: Sheet resistance R_s of Cu(001) thin films measured *in situ* as-deposited (labeled "bare Cu"), after deposition of an Al cap layer with thickness d_{Al} = 0, 0.1, 0.4, and 1.4 nm (labeled "with Al"), during exposure to an increasing O_2 partial pressure of 0.04 - 50 Pa corresponding to 0.1-1.5×10^5 Pa·s, and *ex situ* after exposure to air.

The second set of data points labeled "With Al" are the *in situ* measured R_s values after deposition of Al cap layers on top of the Cu(001). The measured resistance is R_s = 3.91 ± 0.12, 4.05 ± 0.12, and 4.79 ± 0.14 Ω/□ for d_{Al} = 0.1, 0.4, and 1.4 nm, respectively, while there is no data point for the sample labeled "d_{Al} = 0 nm", since this sample has no Al cap. All three capped layers exhibit a considerably larger resistance than before the Al deposition and, more specifically, the resistance increase is more pronounced for larger Al cap thicknesses. This is discussed quantitatively in the following paragraph and Fig. 3, while we subsequently return to finish discussing the data in Fig. 2, particularly the oxygen exposure data.

Fig. 3 is a plot of the change in resistivity $\Delta\rho$ caused by the deposition of an Al cap layer on nominally 10-nm-thick Cu(001), plotted as a function of d_{Al}. The $\Delta\rho$ is determined from the difference in the *in situ* measured R_s with and without Al

cap shown in Fig. 2, and the as-deposited d_{Cu} values from the XRR analyses. Thus, each data point in Fig. 3 is from one distinct sample, as indicated by the colors that correspond to those used in Fig. 2. There is, by definition, no resistivity change in the absence of an Al cap, as indicated by the $\Delta\rho = 0$ data point at $d_{Al} = 0$. The $\Delta\rho$ increases to 0.3, 0.7, and 1.1 μΩcm with increasing $d_{Al} = 0.1$, 0.4, and 1.4 nm. This is attributed to an increasingly diffuse electron surface scattering. That is, the addition of Al on the Cu surface causes a decrease in the specularity p of electron surface scattering, consistent with previous studies on Cu films coated with Pt [33], Ta [7], [33], Ni [25], and Ti [26] overlayers. To illustrate this, the right axis of Fig. 3 shows the change in the surface scattering specularity Δp corresponding to the $\Delta\rho$ on the left axis. The Δp is determined using the approximate form of the FS model for distinct top and bottom surfaces [6], a literature value for the Cu bulk resistivity $\rho_o = 1.7$ μΩcm, a room temperature mean free path $\lambda = 39$ nm [42], and a mean Cu film thickness of 10 nm. The data points for $d_{Al} = 0.1$, 0.4, and 1.4 nm indicate negative $\Delta p = -0.2$, -0.6, and -0.9 values, respectively, indicating that the scattering specularity *decreases* when an Al cap is added. We attribute the decrease in specularity initially to the perturbation of the smooth surface potential [27] caused by the partial coverage of Al atoms for $d_{Al} = 0.1$ nm and then to an increase in the local surface density of states (LSDOS) at the Fermi level E_f with an increasing amount of Al on the Cu surface, similar to what has been reported for the Cu-Ti system [26]. The argument is as follows: The process of an electron scattering into localized surface states effectively corresponds to a completely diffuse surface scattering event, because the localized electron that returns back to the Cu layer exhibits a random momentum that is unaffected by the state prior to the initial scattering event. Since the probability for an electron to scatter into localized surface states is proportional to the LSDOS(E_f) and therefore to d_{Al}, we expect the surface scattering specularity to follow an exponential decay: $p = p_o \exp(-d_{Al}/d_o)$. Here p_o is the scattering specularity of the pristine Cu surface and d_o is a characteristic length that is determined by the cross-section for scattering into localized states and by the LSDOS per Al unit thickness, while the experimental Δp is related to the absolute specularity by $p = p_o + \Delta p$. We use these expressions for data fitting. The result is shown as dotted line in Fig. 3, which describes the measured data well. The fitting procedure yields values for $d_o = 0.43$ nm and $p_o = 0.95$. This latter value for the surface scattering specularity of pristine Cu is larger than what has previously been reported for Cu(001)-vacuum interfaces, with reported values ranging from $p = 0.6 - 0.7$ [7], [25], [26]. This disagreement may be caused by differences in the Cu surface structure (such as smoothness) but may also be attributed to the experimental uncertainty in ρ of 4%, causing an uncertainty in the specularity of ± 0.14 such that $p_o = 0.95 \pm 0.14$. This estimated uncertainty does not include the possibility for interfacial roughening and/or alloying at the Cu-Al interface, which is expected to increase the measured $\Delta\rho$ beyond the effect from diffuse surface scattering and would, in turn, result in a down-correction of p_o. We note that we can also estimate p_o directly from the measured R_s and d_{Cu} for the Cu-layer prior to Al-deposition, using the FS model and assuming completely diffuse scattering at the Cu-MgO interface [6], [7]. This yields $p_o = 1.0$, 0.6, 0.8, and 0.4 for the four samples, with an average $p_o = 0.7 \pm 0.2$. This is smaller than $p_o = 0.95 \pm 0.14$ from the above fitting procedure but is consistent with the preceding arguments and in agreement with previously reported values ranging from 0.6 – 0.7 [7], [25], [26]. Nevertheless, we note that the variation in p_o determined from individual samples is quite large, despite the good sample-to-sample reproducibility of ± 4.6% discussed above. This variability is due to the strong effect that small variations in the measured resistance and layer thickness have on the absolute value of p, which may also be the reason for the large range of reported contradicting p values for some materials systems like Ta coated Cu [7], [28], [30].

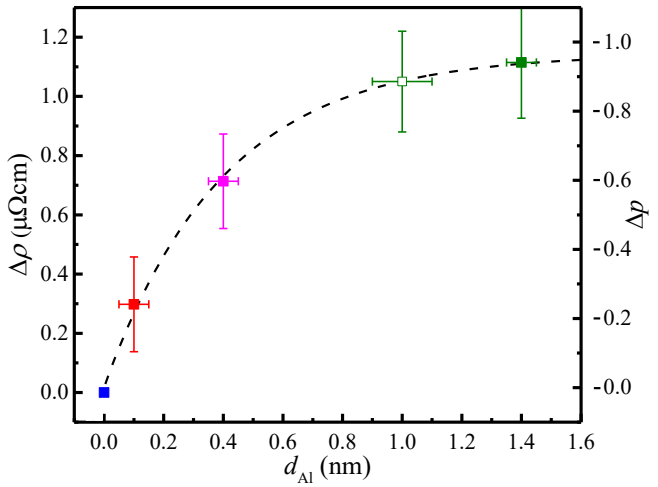

Figure 3: Change in resistivity $\Delta\rho$ due to an Al capping layer with thickness d_{Al} on top of nominally 10-nm-thick Cu(001) films. The right y-axis indicates the corresponding change in the electron surface scattering specularity Δp. The dotted line is the result from curve fitting with an exponential decay in p. The datapoint with the open symbol is for an air-exposed sample which has a 1.0-nm-thick metallic Al layer between the Cu(001) layer and a native AlO_x surface oxide.

We now discuss the effect of oxygen exposure on the measured sheet resistance. Fig. 2 shows the measured R_s as a function of O_2 exposure in units of Pa·s, collected during experiments with a linearly increasing O_2 partial pressure as described in Section II. The plotted range, from 0.1 to 1.5×10^5 Pa·s corresponds to an O_2 partial pressure of 0.04 to 50 Pa, which are reached after 5 and 5990 s of the exposure experiment.

The blue curve in Fig. 2 from the Cu layer without Al cap shows an initial increase in R_s from 3.33 Ω/□ prior to oxygen exposure to a local maximum of $R_s = 3.76$ Ω/□ at an exposure of 1.3 Pa·s, followed by a decrease to $R_s = 3.45$ Ω/□ at 170 Pa·s and an increase to $R_s = 4.16$ and 4.11 Ω/□ at the end of the oxygen exposure experiment and after air exposure, respectively. A similar resistance vs oxygen exposure has previously been reported and discussed [27]. We attribute the initial resistance peak to the adsorption of a partial oxygen monolayer which disturbs the flat surface potential of the original Cu(001) surface, causing increasingly diffuse electron

scattering. The subsequent minimum is likely due to the formation of an ordered adsorbed oxygen layer which results in a relatively flat surface potential and a corresponding large scattering specularity. The final resistance increase is due to chemical oxidation of the Cu surface which causes (1) atomic-scale roughening of the conductive Cu which promotes diffusive electron scattering and (2) consumption of the finite Cu metal thickness by the developing oxide layer, effectively reducing the conductive cross-sectional area as d_{Cu} is reduced from 9.4 to 9.1 nm, as determined by XRR. We note that the slight difference in R_s measured at 1.5×10^5 Pa·s and *ex situ* is within the experimental uncertainty, as these two resistance measurements were done with different 4-point probe setups. The resistivity change from the initial *in situ* measurement to the final *ex situ* measurement corresponds to an overall change in surface specularity of Δp = -0.5, which is comparable to results from previous studies which report values ranging from -0.6 to -0.7 [7], [25], [26].

The red data points in Fig. 2 are from a Cu film coated with 0.1 nm of Al, which corresponds to approximately half a monolayer. The curve qualitatively resembles the one for the uncoated copper and exhibits a local peak of R_s = 3.96 Ω/□ at 2 Pa·s, a minimum of R_s = 3.86 Ω/□ at 55 Pa·s, and reaches R_s = 4.38 and 4.61 Ω/□ at 1.5×10^5 Pa·s and after air exposure, respectively. The curve shape can be explained with initial oxygen adsorption and subsequent chemical surface oxidation, similar to the bare Cu sample discussed above. However, the d_{Al} = 0.1 nm sample has a less pronounced initial peak, which we attribute to a compensating effect. More specifically, while oxygen adsorption causes a disturbance of the flat surface potential and therefore increases diffuse scattering, it also reduces the local surface density of states at the Fermi-level associated with the partial monolayer of Al. Thus, the oxygen adsorption reverses some of the increase in R_s between the "bare Cu" and the "with Al" data points. The final increase in R_s at high exposure is due to chemical oxidation of the Cu surface, confirming that a partial monolayer of Al does not provide oxidative protection of the Cu. This is also consistent with the XRR results which indicate a 1.3 nm thick surface oxide. The overall change in resistivity from *in situ* bare Cu to the *ex situ* air-exposed sample corresponds to a specularity decrease Δp = -0.6, which is comparable to the layer without Al-cap (with Δp = -0.5).

The magenta curve in Fig. 2 from a Cu layer with a 0.4 nm Al cap exhibits a maximum of R_s = 4.21 Ω/□ at 1.4 Pa·s. We note that the edge-feature at 0.1 Pa·s is an artifact of the logarithmic scale in combination with the ± 3 s experimental uncertainty in the starting time for the oxygen exposure and a nearly instantaneous resistance change at the onset of oxygen exposure. The peak at 1.4 Pa·s is similar to that of the previous samples. However, the higher oxygen exposure data are distinctly different: R_s decreases monotonically with increasing oxygen exposure to reach R_s = 3.69 Ω/□ at 1.5×10^5 Pa·s and R_s = 3.66 ± 0.11 Ω/□ after air exposure. This corresponds to a total resistance reduction of 13% which we attribute to an increase in the surface scattering specularity. More specifically, the LSDOS(E_f) decreases as the Al cap layer oxidizes, leading to a decreasing probability to scatter into localized states and, therefore, an increased probability for specular scattering. Similar arguments have previously been reported for Cu layers that were coated with oxidized Ti [26]. We note that this layer exhibits no indication of an increase in R_s at high oxygen exposure, which is in stark contrast to the samples with d_{Al} = 0 and 0.1 nm and suggests that the 0.4 nm Al layer protects the underlying Cu from oxidation. This is consistent with the XRR results presented above, which indicate a completely oxidized Al cap but no CuO_x. The resistivity of the air exposed sample is 3.70 ± 0.13 μΩcm. This is 9.6% higher than the as-deposited bare Cu layer measured in vacuum, but 9.5% lower than the sample after Al cap deposition but prior to oxygen exposure. Quantitative analysis of these values indicates that the surface scattering specularity decreases by Δp = -0.6 due to the addition of the Al cap, but that it increases again by Δp = 0.3 during Al oxidation. This increase is very promising as it indicates the potential to enhance the conductivity of interconnect lines with appropriately chosen barrier layers. This is also demonstrated by a direct comparison of the *ex situ* resistance of this layer (with d_{Al} = 0.4 nm) with the corresponding *ex situ* resistance of the bare Cu layer, showing an 11% resistance decrease and clearly demonstrating that the Al-oxide barrier facilitates specular surface scattering and improved conduction.

The green data points in Fig. 2 from the Cu film with a 1.4 nm Al cap show overall a relatively high sheet resistance which increases slightly from R_s = 4.79 ± 0.14 Ω/□ prior to oxygen exposure to R_s = 5.0 Ω/□ at 2 Pa·s, remains relatively constant from 2 to 10^3 Pa·s, and then continuously decreases to reach an *ex situ* R_s = 4.73 ± 0.14 Ω/□. The slight increase at low exposures qualitatively replicates the increases observed for the other samples while the steep slope at 0.1 Pa·s is, similar to the magenta curve, a plotting artifact. We attribute the decrease at large (> 10^3 Pa·s) exposure to the oxidation of the Al cap. That is, as discussed for the previous sample, oxidation of the Al cap causes a reduction of the LSDOS(E_f) which in turn increases the scattering specularity. However, this effect is much less pronounced for d_{Al} = 1.4 nm than for d_{Al} = 0.4 nm. This is because not the entire 1.4-nm-thick Al cap layer is oxidized. More specifically, as indicated by the XRR analysis, only the top 0.4 nm of the Al layer are oxidized while there remains a 1.0 ± 0.1 nm thick metallic Al layer between the AlO_x surface oxide and the Cu. Thus, the *ex situ* measured resistivity of 4.87 ± 0.17 μΩcm for the d_{Al} = 1.4 nm sample is expected to approximately match that of a Cu layer with a 1.0 nm thick Al cap. To explore this, we determine $\Delta\rho$ = 1.05 μΩcm between the bare Cu and the *ex situ* measurements for this sample and plot it in Fig. 3 as an open square at d_{Al} = 1.0 nm. This point lies along the expected curve, indicating that the oxidized sample matches the expected resistance of a Cu layer with a 1.0 nm thick Al cap and confirming the framework presented in this study that the surface scattering specularity is a direct function of the LSDOS(E_f). Furthermore, this last sample demonstrates that the addition of an Al cap on top of a Cu conductor is only advantageous if the entire cap becomes oxidized, indicating that good process control will be essential when attempting to realize specular surface scattering in interconnect lines.

IV. Conclusions

In situ transport measurements on epitaxial Cu(001) layers show an exponential decrease in the electron surface scattering specularity p when coated with an Al cap with increasing thickness d_{Al}. A combination of XRR analyses and transport measurements during oxygen exposure show that the resistance of bare Cu(001) and of Cu layers coated with a thin (d_{Al} = 0.1 nm) Al cap layer increases due to a decreasing surface scattering specularity caused by a developing Cu surface oxide. In contrast, thicker capping layers with d_{Al} = 0.4 or 1.4 nm (fully or partially oxidized, respectively) suppress oxidation of the underlying Cu, leading to a decreasing resistance. The decrease is due to an increase in the scattering specularity and is most pronounced for the 0.4-nm-thick Al cap which completely oxidizes. The overall results are explained by electron scattering into localized surface states, which effectively results in diffuse surface scattering and a resistance increase. That is, an increasing Al cap thickness causes an increasing LSDOS(E_f) and an increasing resistance, while Al oxidation reduces the LSDOS(E_f) and lowers the resistance. These results suggest that insulating liner layers promote specular surface scattering and therefore facilitate narrow high-conductivity interconnects.

References

[1] J. Kelly, J. H.-C. Chen, H. Huang, C. K. Hu, E. Liniger, R. Patlolla, B. Peethala, P. Adusumilli, H. Shobha, T. Nogami, T. Spooner, E. Huang, D. Edelstein, D. Canaperi, V. Kamineni, F. Mont, and S. Siddiqui, "Experimental study of nanoscale Co damascene BEOL interconnect structures," in *2016 IEEE International Interconnect Technology Conference / Advanced Metallization Conference (IITC/AMC)*, May. 2016, pp. 40–42, doi: 10.1109/IITC-AMC.2016.7507673.

[2] J. S. Chawla, S. H. Sung, S. A. Bojarski, C. T. Carver, M. Chandhok, R. V. Chebiam, J. S. Clarke, M. Harmes, C. J. Jezewski, M. J. Kobrinski, B. J. Krist, M. Mayeh, R. Turkot, and H. J. Yoo, "Resistance and electromigration performance of 6 nm wires," in *2016 IEEE International Interconnect Technology Conference / Advanced Metallization Conference (IITC/AMC)*, May. 2016, pp. 63–65, doi: 10.1109/IITC-AMC.2016.7507682.

[3] N. A. Lanzillo, H. Dixit, E. Milosevic, C. Niu, A. V Carr, P. Oldiges, M. V Raymond, J. Cho, T. E. Standaert, and V. K. Kamineni, "Defect and grain boundary scattering in tungsten: A combined theoretical and experimental study," *J. Appl. Phys.*, vol. 123, no. 15, p. 154303, Apr. 2018, doi: 10.1063/1.5027093.

[4] D. Gall, "Metals for Low-Resistivity Interconnects," in *2018 IEEE International Interconnect Technology Conference (IITC)*, Jun. 2018, pp. 157–159, doi: 10.1109/IITC.2018.8456810.

[5] E. Milosevic, S. Kerdsongpanya, A. Zangiabadi, K. Barmak, K. R. Coffey, and D. Gall, "Resistivity size effect in epitaxial Ru(0001) layers," *J. Appl. Phys.*, vol. 124, no. 16, p. 165105, Oct. 2018, doi: 10.1063/1.5046430.

[6] J. S. Chawla, F. Gstrein, K. P. O'Brien, J. S. Clarke, and D. Gall, "Electron scattering at surfaces and grain boundaries in Cu thin films and wires," *Phys. Rev. B*, vol. 84, no. 23, p. 235423, Dec. 2011, doi: 10.1103/PhysRevB.84.235423.

[7] J. S. Chawla and D. Gall, "Specular electron scattering at single-crystal Cu(001) surfaces," *Appl. Phys. Lett.*, vol. 94, no. 25, p. 252101, Jun. 2009, doi: 10.1063/1.3157271.

[8] M. César, D. Gall, and H. Guo, "Reducing Grain-Boundary Resistivity of Copper Nanowires by Doping," *Phys. Rev. Appl.*, vol. 5, no. 5, p. 054018, May 2016, doi: 10.1103/PhysRevApplied.5.054018.

[9] M. César, D. Liu, D. Gall, and H. Guo, "Calculated Resistances of Single Grain Boundaries in Copper," *Phys. Rev. Appl.*, vol. 2, no. 4, p. 044007, Oct. 2014, doi: 10.1103/PhysRevApplied.2.044007.

[10] K. Barmak, A. Darbal, K. J. Ganesh, P. J. Ferreira, J. M. Rickman, T. Sun, B. Yao, A. P. Warren, and K. R. Coffey, "Surface and grain boundary scattering in nanometric Cu thin films: A quantitative analysis including twin boundaries," *J. Vac. Sci. Technol. A Vacuum, Surfaces, Film.*, vol. 32, no. 6, p. 061503, Nov. 2014, doi: 10.1116/1.4894453.

[11] T.-H. Kim, X.-G. Zhang, D. M. Nicholson, B. M. Evans, N. S. Kulkarni, B. Radhakrishnan, E. A. Kenik, and A.-P. Li, "Large Discrete Resistance Jump at Grain Boundary in Copper Nanowire," *Nano Lett.*, vol. 10, no. 8, pp. 3096–3100, Aug. 2010, doi: 10.1021/nl101734h.

[12] J. M. Rickman and K. Barmak, "Simulation of electrical conduction in thin polycrystalline metallic films: Impact of microstructure," *J. Appl. Phys.*, vol. 114, no. 13, p. 133703, Oct. 2013, doi: 10.1063/1.4823985.

[13] P. Y. Zheng, T. Zhou, B. J. Engler, J. S. Chawla, R. Hull, and D. Gall, "Surface roughness dependence of the electrical resistivity of W(001) layers," *J. Appl. Phys.*, vol. 122, no. 9, p. 095304, Sep. 2017, doi: 10.1063/1.4994001.

[14] Y. Ke, F. Zahid, V. Timoshevskii, K. Xia, D. Gall, and H. Guo, "Resistivity of thin Cu films with surface roughness," *Phys. Rev. B*, vol. 79, no. 15, p. 155406, Apr. 2009, doi: 10.1103/PhysRevB.79.155406.

[15] T. Zhou, P. Zheng, S. C. Pandey, R. Sundararaman, and D. Gall, "The electrical resistivity of rough thin films: A model based on electron reflection at discrete step edges," *J. Appl. Phys.*, vol. 123, no. 15, p. 155107, Apr. 2018, doi: 10.1063/1.5020577.

[16] W. Zhang, S. H. Brongersma, Z. Li, D. Li, O. Richard, and K. Maex, "Analysis of the size effect in electroplated fine copper wires and a realistic assessment to model copper resistivity," *J. Appl. Phys.*, vol. 101, no. 6, p. 063703, Mar. 2007, doi: 10.1063/1.2711385.

[17] M. H. van der Veen, N. Jourdan, V. V. Gonzalez, C. J. Wilson, N. Heylen, O. V. Pedreira, H. Struyf, K. Croes, J. Bommels, and Z. Tokei, "Barrier/liner stacks for scaling the Cu interconnect metallization," in *2016 IEEE International Interconnect Technology Conference / Advanced Metallization Conference (IITC/AMC)*, May. 2016, pp. 28–30, doi: 10.1109/IITC-AMC.2016.7507649.

[18] K. Fuchs and N. F. Mott, "The conductivity of thin metallic films according to the electron theory of metals," *Math. Proc. Cambridge Philos. Soc.*, vol. 34, no. 01, p. 100, Jan. 1938, doi: 10.1017/S0305004100019952.

[19] E. H. Sondheimer, "The mean free path of electrons in metals," *Adv. Phys.*, vol. 1, no. 1, pp. 1–42, Jan. 1952, doi: 10.1080/00018735200101151.

[20] J. S. Chawla and D. Gall, "Epitaxial Ag(001) grown on MgO(001) and TiN(001): Twinning, surface morphology, and electron surface scattering," *J. Appl. Phys.*, vol. 111, no. 4, p. 043708, Feb. 2012, doi: 10.1063/1.3684976.

[21] G. Kästle, H.-G. Boyen, A. Schröder, A. Plettl, and P. Ziemann, "Size effect of the resistivity of thin epitaxial gold films," *Phys. Rev. B*, vol. 70, no. 16, p. 165414, Oct. 2004, doi: 10.1103/PhysRevB.70.165414.

[22] M. S. P. Lucas, "The effects of surface layers on the conductivity of gold films," *Thin Solid Films*, vol. 2, no. 4, pp. 337–352, Nov. 1968, doi: 10.1016/0040-6090(68)90039-4.

[23] J. R. Sambles, K. C. Elsom, and D. J. Jarvis, "The Electrical Resistivity of Gold Films," *Philos. Trans. R. Soc. A Math. Phys. Eng. Sci.*, vol. 304, no. 1486, pp. 365–396, Mar. 1982, doi: 10.1098/rsta.1982.0016.

[24] E. Milosevic, S. Kerdsongpanya, M. McGahay, A. Zangiabadi, and K. Barmak, "ELectron-Surface Scattering in Epitaxial Co(0001) Films," *Manuscrip Prep.*, 2018.

[25] P. Y. Zheng, R. P. Deng, and D. Gall, "Ni doping on Cu surfaces: Reduced copper resistivity," *Appl. Phys. Lett.*, vol. 105, no. 13, p. 131603, Sep. 2014, doi: 10.1063/1.4897009.

[26] P. Zheng, T. Zhou, and D. Gall, "Electron channeling in TiO 2 coated Cu layers," *Semicond. Sci. Technol.*, vol. 31, no. 5, p. 055005, May 2016, doi: 10.1088/0268-1242/31/5/055005.

[27] J. S. Chawla, F. Zahid, H. Guo, and D. Gall, "Effect of O2 adsorption on electron scattering at Cu(001) surfaces," *Appl. Phys. Lett.*, vol. 97, no. 13, p. 132106, Sep. 2010, doi: 10.1063/1.3489357.

[28] H. Kitada, T. Suzuki, S. Akiyama, and T. Nakamura, "Influence of Titanium Liner on Resistivity of Copper Interconnects," *Jpn. J. Appl. Phys.*, vol. 48, no. 4, p. 04C026, Apr. 2009, doi: 10.1143/JJAP.48.04C026.

[29] M. Shimada, M. Moriyama, K. Ito, S. Tsukimoto, and M. Murakami, "Electrical resistivity of polycrystalline Cu interconnects with nano-scale linewidth," *J. Vac. Sci. Technol. B Microelectron. Nanom. Struct.*, vol. 24, no. 1, p. 190, 2006, doi: 10.1116/1.2151910.

[30] A. Sakata, S. Kato, Y. Yano, H. Toyoda, T. Kawanoue, M. Hatano, J. Wada, N. Yamada, T. Oki, H. Yamaguchi, N. Nakamura, K. Higashi, M. Yamada, T. Fujimaki, and M. Hasunuma, "Copper Line Resistance Control and Reliability Improvement by Surface Nitridation of Ti barrier Metal," in *2008 International Interconnect Technology Conference*, Jun. 2008, no. 2, pp. 165–167, doi: 10.1109/IITC.2008.4546956.

[31] D. Choi, C. S. Kim, D. Naveh, S. Chung, A. P. Warren, N. T. Nuhfer, M. F. Toney, K. R. Coffey, and K. Barmak, "Electron mean free path of tungsten and the electrical resistivity of epitaxial (110) tungsten films," *Phys. Rev. B*, vol. 86, no. 4, p. 045432, Jul. 2012, doi: 10.1103/PhysRevB.86.045432.

[32] T. Sun, B. Yao, A. P. Warren, K. Barmak, M. F. Toney, R. E. Peale, and K. R. Coffey, "Dominant role of grain boundary scattering in the resistivity of nanometric Cu films," *Phys. Rev. B*, vol. 79, no. 4, p. 041402, Jan. 2009, doi: 10.1103/PhysRevB.79.041402.

[33] S. M. Rossnagel and T. S. Kuan, "Alteration of Cu conductivity in the size effect regime," *J. Vac. Sci. Technol. B Microelectron. Nanom. Struct.*, vol. 22, no. 1, p. 240, 2004, doi: 10.1116/1.1642639.

[34] B. Wang, S. Kerdsongpanya, M. E. McGahay, E. Milosevic, P. Patsalas, and D. Gall, "Growth and properties of epitaxial Ti 1− x Mg x N(001) layers," *J. Vac. Sci. Technol. A*, vol. 36, no. 6, p. 061501, Nov. 2018, doi: 10.1116/1.5049957.

[35] K. Wefers and C. Misra, "Oxides and Hydroxides of Aluminum. Alcoa Technical Paper No. 19," 1987.

[36] R. Deng, B. D. Ozsdolay, P. Y. Zheng, S. V. Khare, and D. Gall, "Optical and transport measurement and first-principles determination of the ScN band gap," *Phys. Rev. B*, vol. 91, no. 4, p. 045104, Jan. 2015, doi: 10.1103/PhysRevB.91.045104.

[37] P. Zheng, B. D. Ozsdolay, and D. Gall, "Epitaxial growth of tungsten layers on MgO (001)," *J. Vac. Sci. Technol. A Vacuum, Surfaces, Film.*, vol. 33, no. 6, pp. 061505-1–7, 2015.

[38] J. S. Chawla, X. Y. Zhang, and D. Gall, "Epitaxial TiN(001) wetting layer for growth of thin single-crystal Cu(001)," *J. Appl. Phys.*, vol. 110, no. 4, p. 043714, Aug. 2011, doi: 10.1063/1.3624773.

[39] J. M. Purswani and D. Gall, "Surface morphological evolution during annealing of epitaxial Cu(001) layers," *J. Appl. Phys.*, vol. 104, no. 4, p. 044305, Aug. 2008, doi: 10.1063/1.2968440.

[40] S. Cazottes, Z. L. Zhang, R. Daniel, J. S. Chawla, D. Gall, and G. Dehm, "Structural characterization of a Cu/MgO(001) interface using CS-corrected HRTEM," *Thin Solid Films*, vol. 519, no. 5, pp. 1662–1667, Dec. 2010, doi: 10.1016/j.tsf.2010.09.017.

[41] L. Nguyen, T. Hashimoto, D. N. Zakharov, E. A. Stach, A. P. Rooney, B. Berkels, G. E. Thompson, S. J. Haigh, and T. L. Burnett, "Atomic-scale insights into the oxidation of aluminum," ACS Appl. Mater. Interfaces, vol. 10, no. 3, pp. 2230–2235, 2018, doi: 10.1021/acsami.7b17224.

[42] J. M. Purswani and D. Gall, "Electron scattering at single crystal Cu surfaces," *Thin Solid Films*, vol. 516, no. 2–4, pp. 465–469, Dec. 2007, doi: 10.1016/j.tsf.2007.07.146.